Available online at www.sciencedirect.com
ScienceDirect
Ceramics International 36 (2010) 107–113
CERAMICS INTERNATIONAL
www.elsevier.com/locate/ceramint

Preparation and properties of bimodal porous apatite ceramics through slip casting using different hydroxyapatite powders

Yin Zhang [a,*], Yoshiyuki Yokogawa [b], Xia Feng [c], Yaqiu Tao [a], Yuanqiang Li [a]

[a] *Nanjing University of Technology, NO.5 Xinmofan Road, Nanjing, China*
[b] *Osaka City University, 3-3-138 Sugimoto-cho, Sumiyoshi-ku, Osaka 558-8585, Japan*
[c] *The Fraternity Hospital of Nanjing Red Cross, NO.113 yuhuaxi Road, Nanjing, China*

Received 24 February 2009; received in revised form 10 March 2009; accepted 4 July 2009
Available online 11 August 2009

Abstract

A bimodal porous hydroxyapatite (HAp) body with high flexural strength was prepared through slip casting. The effect of different particle sizes on the flexural strength and microstructure of three different types of hydroxyapatite (HAp) powders was studied. The powder characteristic of laboratory-synthesized HAp powder (L-HAp) was obtained through a wet-milling method, drying and heating of a mixture of calcium hydrogen phosphate di-hydrate and calcium carbonate. The median particle size of L-HAp was 0.34 μm, and the specific surface area was 38.01 m^2/g. The commercial HAp had median particle sizes for the K-HAp (Kishida chemical Co. Ltd., K-HAp) and T-HAp (Taihei chemical Co. Ltd., T-HAp) of 1.13 and 3.65 μm, and specific surface areas of 11.62 and 6.23 m^2/g, respectively. The different powder characteristics affected the slip characteristics, and the flexural strength and microstructure of the sintered porous HAp bodies were also different. The flexural strengths of the porous HAp ceramics prepared by heating at 1200 °C for 3 h in air were 17.59 MPa for L-HAp with a porosity of 60.48%, 3.92 MPa for commercial K-HAp with a porosity of 79.37%, and 4.55 MPa for commercial T-HAp with a porosity of 76.46%.

Keywords: Hydroxyapatite; Porous material; Bimodal; Different powders; Properties

1. Introduction

Bioactive ceramics such as hydroxyapatite (HAp, with Ca/P = 1.67) may provide a three-dimensional guideline for bone frame, which facilitates bone in-growth and subsequent positional stability. In recent years, attention has been particularly directed to the fabrication of bio-ceramics with deliberately introduced porous configurations to allow tissue infiltration, which enhances the implant-tissue attachment [1–3]. In recent years, attention has been particularly directed to the fabrication of bio-ceramics with deliberately introduced porous configurations to allow tissue infiltration, which enhances the implant-tissue attachment [4–6]. In a porous form, HAp ceramics can be colonized by bone tissues with the same characteristics as peri-implanted tissues [7]. Macropores of 200 μm or more in size favor bone in-growth, and bone cells colonize and proliferate inside the macropores through the interconnections between the macropores. If micropores of around 1 μm are interconnected, these can promote the assimilation to bone as well as bone formation [6–8], due to blood circulation and extra-cellular liquid exchange, prior to bone in-growth. Therefore, bimodal-type porous HAp materials having both macropores of 200 μm or more and micropores of 1 μm in size are expected to allow bone in-growth and early bone assimilation. The flexural strength of the HAp dense ceramics was around 150 MPa [9,10], but that of porous HAp ceramics remarkably decreased with an increase of porosity. The flexural strength of the porous HAp ceramics with a porosity of 60% is, generally around 8 MPa [9,10]. Various methods to impart porosity to a ceramic body are known, mainly based on the admixing of a foreign combustible organic material that is burnt out during firing [4–11,12]. The coating of polymer foams with a ceramic slip is the most widespread processing approach for producing an open-pore structure. Characteristics of the particles such as specific surface area, and electrostatic surface charge influence the stabilization and deflocculation behaviour of powder particle dispersions in a slip, and the slip characteristics strongly influence the density of

* Corresponding author. Tel.: +86 25 83587787; fax: +86 25 83240205.
E-mail address: zhang.512@gmail.com (Y. Zhang).

0272-8842/$36.00
doi:10.1016/j.ceramint.2009.07.008

the green body and the mechanical properties of the sintered body. High solid content in a slip is favorable to yielding the highly dense green body resulting in a high-strength sintered body. The high viscosity of a slip appears above a certain specific surface area [13]. Generally powders with high specific surface area are easily sintered, but powders whose characteristics such as specific surface area, size, and morphology are suitable for a elaboration of a suspension with high powder loading.

Here, the preparation of bimodal porous hydroxyapatite ceramics through slip casting using different hydroxyapatite particle size and shapes on the properties of HAp porous sintered body is discussed. As a result, it is thought that it is possible to serve as a reference for the synthesis of a different structure porous body.

2. Materials, methods and measurements

Materials a mixture of calcium hydrogen phosphate dihydrate ($CaHPO_4{\cdot}2H_2O$) and calcium carbonate ($CaCO_3$) at the mole ratio of 3:2 was added to a 90 wt% water solution to make a slurry. The slurry was mechanically agitated using zirconia balls in a zirconia pot mill at 50 rpm for 24 h at room temperature. The resulting slurry was then dried, and heat-treated in air at 720 °C for 8 h to produce a fine HAp powder (L-HAp).

Commercial K-HAp (Kishida chemical Co. Ltd., K-HAp) and T-HAp (Taihei chemical Co. Ltd., T-HAp) powders were used for studying in the as-received state.

Methods the slip was obtained by adding the HAp powder to a solution of deflocculant (Seluna D-305 from Chukyo Oils and Fats Co. Ltd.) diluted 10 times with water and 0.5 wt% of foaming agent (Emma-RU D-3-D of Kao Corp.). The solid content of the slip was varied from 48.0, 62.5 and 65.0 wt%, and that of the deflocculant was 1.5 wt%. The specimen was obtained by dipping a polyurethane block (medium pore size type supplied by Ube Industries Inc.) into the slip, and then drying it under vacuum. The dried specimens were heated at a rate of 0.5 °C/min to 250 °C, then kept at 250 °C for 30 min to decompose the deflocculant. They were subsequently heated again at the rate of 3 °C/min to 1200 °C, respectively, fired for 3 h at the given temperature, then cooled to room temperature at the rate of 3 °C/min to yield 3 samples.

Measurements the crystal phase of the synthesized powder and sintered powders were each examined by an X-ray powder diffraction method using an X-ray diffractometer at 40 kV and a 20 mA Cu target with CuKα radiation (wavelength = 1.54056 Å) (MAC Science MXP^3). Identification of phases was achieved by comparing the diffraction patterns with ICDD (JCPDS) standards [15]. Data were collected over the 2θ range 10–60° with a step size of 0.02° and a count time of 5 s.

Fourier transform infrared (FT-IR) analyses (Jasco, MFT-2000) using KBr were done. The Ca/P molar ratio of the synthesized powder was by ICP (Seiko, ISM7000s). Average particle diameter of the synthesized powder was calculated by a centrifugal sedimentation method with a 0.2% solution of sodium pyrophosphate as a dispersion medium and using SA-CP3 of Shimadzu Co. The specific surface area (SSA) of the powders was determined by the Brunauer–Emmett–Teller (BET) methods using a surface area analyzer (Flow SOBU II 2300 type of Shimadzu Co.). The rheological properties of the slip were characterized using a digital viscometer (DV-II+ of Brook field). The pH value of the slurry was measured using pH meter. The densities of HAp porous bodies were obtained by the water immersion method based on the Archimedean principle. All densities were quoted as a percentage of the theoretical density of HAp, 3.156 g/cm^3 [14]. The pore size distribution was measured using mercury intrusion porosimetry (AutoPore IV 9500 of Shimadzu Co.). The bending strengths of both the porous and dense HAp sintered bodies were measured by a three-point bending method in which the supporting parts were set 40 mm from one another with a crosshead speed of 0.5 mm/min. Scanning electron microscopy (SEM) and EDX analyses of the powders and sintered powders were performed using a Hitachi S-3000 SEM, and Horiba EMAX-2200 X-ray analyzer.

3. Results and discussions

3.1. Powder characterization

The results of the ICP analysis showed that the Ca/P molar ratio of L-HAp, K-HAp and T-HAp were 1.668, 1.665 and 1.675, respectively. Within the accuracy of the analysis, both samples had Ca/P molar ratios comparable to a stoichiometry of 1.67. The average particle diameter of the wet-milled [15] synthesized powders calcined at 720 °C (L-HAp), commercial K-HAp and T-HAp, were 0.32, 1.13 and 3.65 μm, respectively, and the specific surface areas were 38.1, 11.62 and 6.23 m^2/g, respectively. The characterization of Ca/P molar ratio, Particle size and Specific surface area in the three samples are listed in Table 1.

XRD analysis showed that three samples of L-HAp, K-HAp and T-HAp produced only peaks that corresponded to stoichiometric HAp [16]. This is further evidence that the material created in this study was single-phase and did not decompose to secondary phases on sintering/heating (Fig. 1). The K-HAp sample was poorly crystalline, as shown by the broad diffraction peaks, which is characteristic of HAp prepared by an aqueous precipitation route [17,18]. In contrast, the L-HAp and T-HAp powders produced a diffraction pattern that corresponded to a crystalline material, with narrow diffraction peaks, which is characteristic of a powder that has been heat-treated.

Structural changes of the HAp powders were analyzed by FT-IR, as shown in Fig. 2. In L-HAp and K-HAp powders, P-O

Table 1
The characterization of Ca/P molar ratio, particle size and specific surface area in different HAp powders.

Sample	Ca/P	Particle size (μm)	Specific surface area (m^2/g)
L-HAp	1.668 ± 0.006	0.34 ± 0.05	38.01 ± 0.80
K-HAp	1.665 ± 0.004	1.17 ± 0.10	11.62 ± 0.03
T-HAp	1.675 ± 0.005	3.65 ± 0.33	6.23 ± 0.69

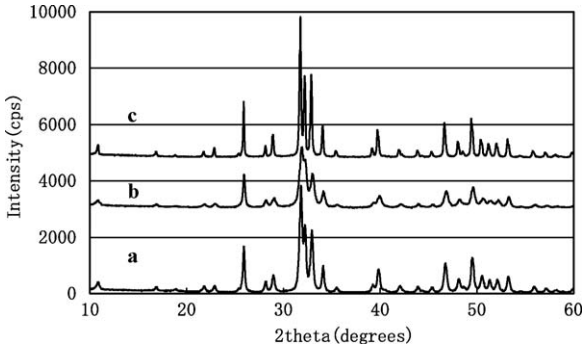

Fig. 1. XRD patterns of the HAp powders (a) L-HAp, (b) K-HAp and (c) T-HAp.

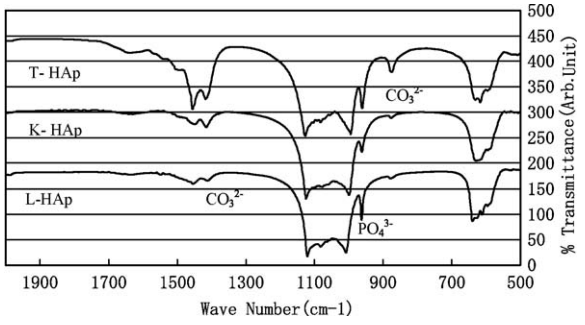

Fig. 2. Infrared absorption spectra of the powders: L-HAp, K-HAp and T-HAp.

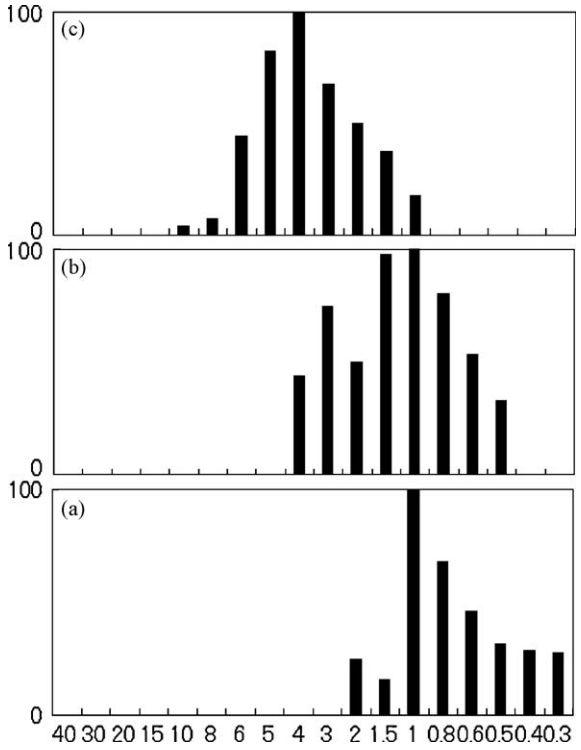

Fig. 4. The typical particle size distributions of (a) the powders of L-HAp, (b) the powders of K-HAp and (c) the powders of T-HAp.

bands (500–600 and 900–1000 cm^{-1}) showed and a weak CO_3^{2-} band was observed indicating formation of the typical apatite structure. In the T-HAp powder, the CO_3^{2-} band (870 and 1460 cm^{-1}) became sharp and stronger than the L-HAp and K-HAp, indicating that the CO_3^{2-} remained in the form of apatite [19]. Moreover, the O–H stretching mode was observed at 640 cm^{-1}, confirming the formation of characteristic apatite structure, containing a hydroxyl group. The P–O band became sharp and strong in L-HAp and T-HAp indicating an improvement in the atomic arrangement of the apatite structure.

The morphology of the three powders is illustrated in the SEM micrographs, Fig. 3. The L-HAp powder appears as a dumbbell shape with a higher surface area, the K-HAp powder appears as a needle shape, and the T-HAp powder appears a cylinder shape with a lower surface area. Although the chemical and phase compositions of the three powders are similar, the characterization of the three powders including the size distribution, surface area and the morphology were very different. And these differences must be come up with the synthesis condition and method of the different powder.

The particle size distributions of the sample powders are illustrated in Fig. 4. The particle size of L-HAp powders was distributed from 0.3 to 2.0 μm; that of K-HAp powders was distributed from 0.5 to 4.0 μm; and that of T-HAp powders was distributed from 1.0 to 10.0 μm.

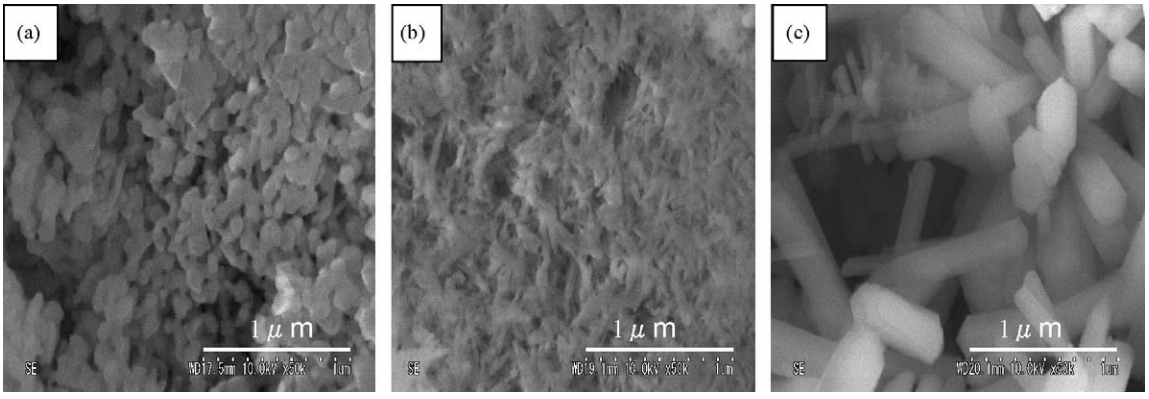

Fig. 3. SEM photo of powders: (a) L-HAp, (b) K-HAp and (c) T-HAp.

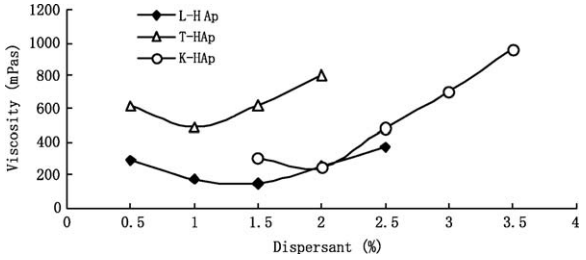

Fig. 5. Viscosity measured at a shear rate of 10.2 s^{-1}, plotted as function of dispersant concentration for HAp suspension containing 48.0, 62.5 and 65.0%.

3.2. Slip characterization and foaming

Fig. 5 shows the effect of dispersant concentration on the viscosity of suspensions at various loadings of HAp powder. The viscosity can be seen to approach a minimum for all solid loadings. The behaviour has been explained elsewhere [20,21].

All the slips prepared in this work revealed a shear thinning or pseudoplastic behaviour. This behaviour is characterized by the decrease in viscosity at increasing shear rates and is typically found in the dispersion of HAp suspensions containing a high percentage of solids. In the fabrication of ceramic foams, a slight pseudoplasticity can favor the generation of the foam since lower viscosities are obtained under shearing, and, under static conditions, can significantly improve the foam stability since the viscosity increase delays the collapse of fluid films around the bubbles. Particle size and powder concentration greatly influence the rheological behaviour of a slip [22]. To obtain an HAp slip with a reasonably low viscosity for a solids loading, L-HAp, K-HAp and T-HAp powder concentration was 48.0, 62.5 and 65.0 wt%, respectively, with 1.5, 2.0 and 1.0 wt% dispersant respectively. The viscosity of the slip containing 48.0, 62.5 and 65.0 wt% HAp powders shows similar behaviour versus the different deflocculant concentrations.

The rheology of the slips displayed in Fig. 6(a) appears to be typical of pseudoplastic fluids. The behaviour can be confirmed by the variation of shear stress against shear rate observed in the curves of Fig. 6(b). The shear stress of a slip prepared with the powder of L-HAp with a larger specific surface area was smaller than that of the powder of commercial HAp with a smaller specific surface area. Similarly, the viscosity of a slip prepared with the powder of L-HAp with a larger specific surface area was smaller than that of powder of commercial HAp with a smaller specific surface area.

The optimum value for the minimum viscosity in the present HAp slip with respect to its solid loading was 48.0, 62.5 and 65.0 wt%, respectively, which is relatively low compared to that reported in other papers [23], due most likely to the large surface area of the HAp used to prepare the slip [13].

Slip casting is common as a shaping/forming process, and many studies on the method suitable for forming a high density HAp body were reported [11–13]. To improve the density of the HAp sinter, suspensions with a high HAp concentration were prepared using a deflocculant. The nature of the surface of HAp particles influenced the rheological behaviour of the slurries. An increase of viscosity appears above a certain specific surface

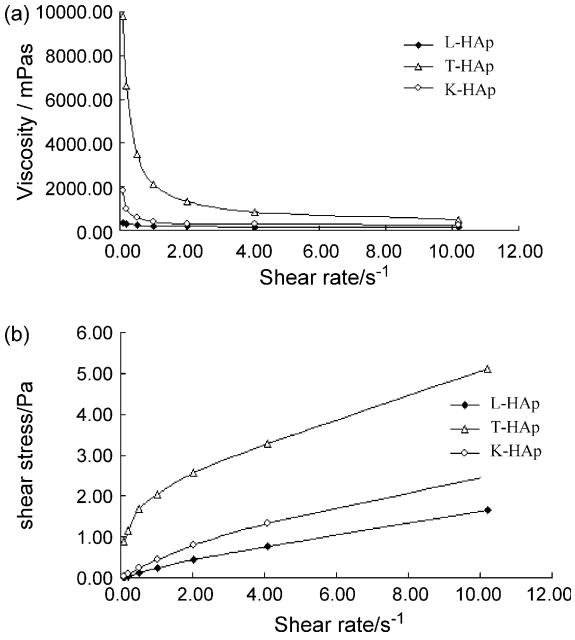

Fig. 6. Flow behaviour of suspensions containing L-HAp 48.0%, K-HAp 62.5% and T-HAp 65.0%. Plots of (a) viscosity and (b) shear stress against shear rate are shown.

area over the range of 10–15 m^2/g [13]. Therefore, suspensions with high HAp concentration can be obtained using a HAp powder of relatively low specific surface area [13]. Here fine HAp powders with high specific surface area were applied, so the solid loading at the minimum viscosity was relatively low.

The slip rheology is important because the process involves casting. In common with other casting operations, very fluid systems are required in order to enable easy filling of high complexity shapes. The high viscosity characteristics of slip systems at low shear rates can thus be a critical factor for the production of complex shaped foamed bodies.

The specimen obtained by casting polyurethane foam with 0.5 wt% into a slip, and drying it under vacuum, was heated at 1200 °C, for 3 h. The purpose of the heat-treatment process is to drive off the volatiles and the urethane foam in order to form a porous network.

3.3. Porous body properties

3.3.1. Porous body characterization

Fig. 7 shows the porosity, and relative density of L-HAp, K-HAp and T-HAp porous ceramics. The porosity of L-HAp, K-HAp and T-HAp porous HAp sintered body were 60.48%, 79.37%, and 76.46%, respectively. The relative density of L-HAp, K-HAp and T-HAp porous HAp sintered body were 35.77%, 17.34% and 21.0%, respectively. The relative density of the specimens decreased with an increase of the porosity of bimodal-type porous HAp ceramics and depends on its pore structure, such as the volume ratio of macropores to micropores.

3.3.2. Pore structure

Fig. 8 shows the pore size distribution of the HAp sintered body prepared by heating the foam in an HAp slip. The peak

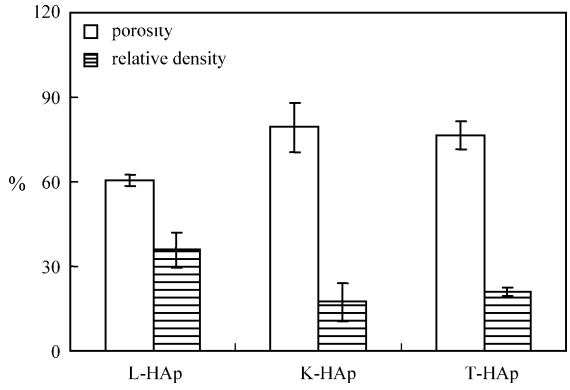

Fig. 7. The porosity and relative density of L-HAp, K-HAp and T-HAp porous ceramics after heat treatment at 1200 °C. for 3 h.

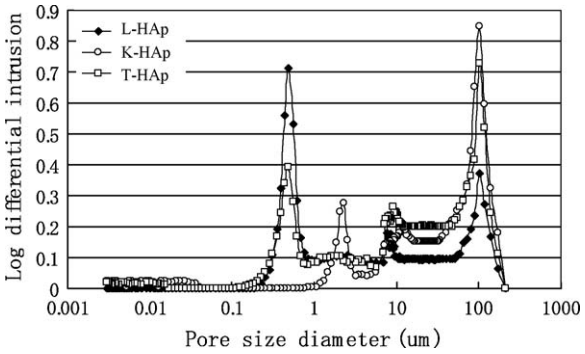

Fig. 8. Pore size distribution of HAp sintered body prepared by heating the foam dipped in HAp slip with 1.5 wt% of deflocculant and 0.5 wt% of foaming reagent.

height of the distribution curve indicates the number of pores. A vast number of micropores, generally in the size range of 0.5–20 μm, and macropores of several dozens μm in size can be detected using a mercury porosimeter. The number of pores in a specimen obtained from a slip containing 62.5 wt% HAp powder (K-HAp) heated at 1200 °C was greater than that of the samples 48.0 wt% (L-HAp) and 65.0 wt% HAp (T-HAp) powders heated at the same 1200 °C.

For the specimen from a slip containing 62.5 and 65.0 wt% HAp powder, the peak intensities of the pore size distribution curve were higher in a macropore situation. However, for the specimen from a slip containing 48.0 wt% HAp powder, the peak intensities of the pore size distribution curve were higher in a micropore situation. The porous size in a micropore for specimen K-HAp was larger then the samples L-HAp and T-HAp.

Care must be taken to analyze the data obtained by mercury porosimetry, because the results may differ from the real pore size distribution of the samples. The SEM observation reveals that HAp foams were typically composed of large spherical

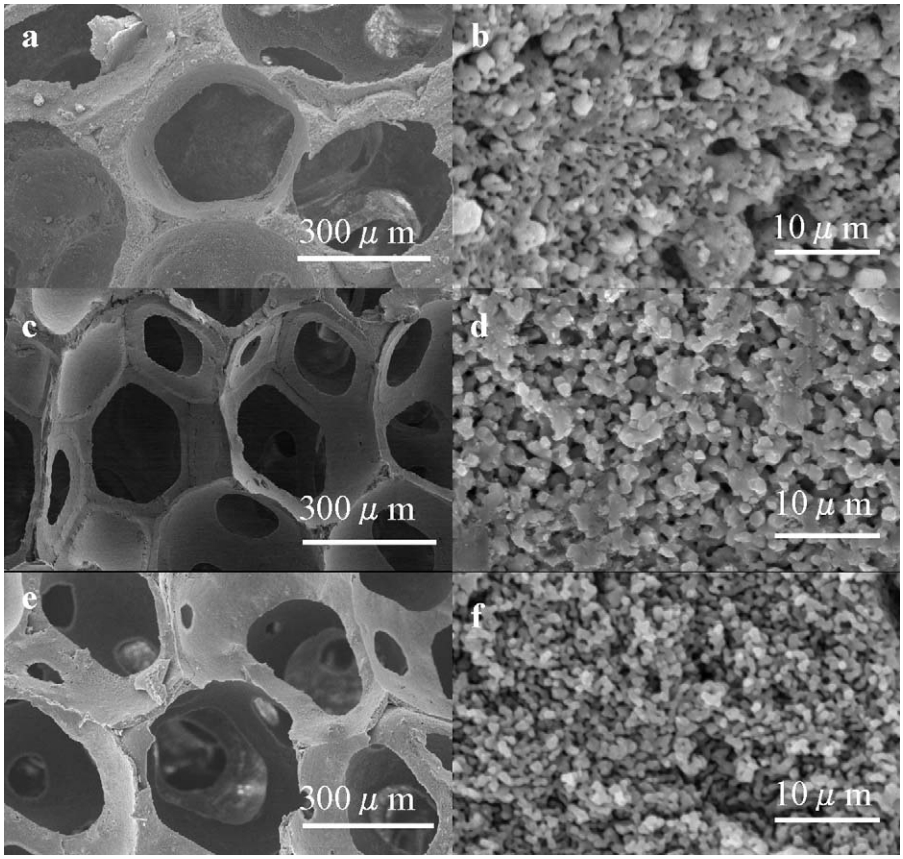

Fig. 9. SEM micrographs of HAp sintered body obtained by heating at 1200 °C the foam dipped in 48.0 (a, b), 62.5 (c, d), and 65.0 (e, f) wt% HAp slip with 1.5 wt% of deflocculant and 0.5 wt% of foaming reagent. (a), (c) and (e) are the macropores; (b), (d) and (f) are the micropores.

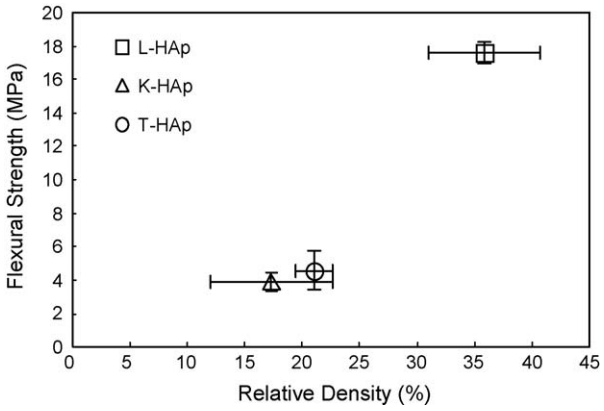

Fig. 10. Relationship between relative density and flexural strength of the HAp sintered body prepared by heating the foam dipped in 48.0, 62.5 and 65.0 wt% HAp slip with 1.5 wt% of deflocculant and 0.5 wt% of foaming reagent at 1200 °C.

pores with small interconnecting rectangular pores. The large spherical pore size is approximately 300 μm. A large number of small pores, generally in the size range of 0.1–20 μm, can be observed, distributed around the large spherical pore walls. These pores appear to be highly interconnected as confirmed by the mercury porosimetry. A large number of small pores with a size of several μm or smaller was observed in the specimen obtained by heating at 1200 °C, and these might have been formed by the addition of the surfactant.

From Figs. 9 and 10, we can find micropore of K-HAp sintered body is different from L-HAp and T-HAp sintered body. The size of micropore in K-HAp sintered body is larger than L-HAp and T-HAp sintered body. That is because of primary K-HAp powder was poorly crystalline, as shown at Fig. 1. When K-HAp body was heated at 1200 °C for 3 h, the change of K-HAp particles is hugest than L-HAp and T-HAp. Therefore, its microstructure is different from L-HAp and T-HAp sintered body.

The large spherical pores and interconnecting pore sizes are large enough for cells to pass through and proliferate, and the pore size is small enough for nutrients to circulate through in order to induce cell growth [14,24,25]. Therefore, the bimodal pore structure of the HAp sintered body as obtained in this study should provide a more suitable bone filling material for biomedical applications.

3.3.3. Mechanical properties

The flexural strength of the porous HAp ceramic was measured using a three-point fixture. The test of rectangular pieces using HAp sintered bodies prepared by heating the foam dipped in the L-HAp 48.0, K-HAp 62.5 wt% and T-HAp 65.0 wt% HAp slip with 1.5 wt% deflocculant and 0.5 wt% foaming reagent yielded flexural strengths of 17.59, 3.92 and 4.55 MPa for the 1200 °C sintering temperatures, respectively. The porosity of these porous HAp sintered body were 60.48%, 79.37%, and 76.46%, respectively. The flexural strength obtained from 48.0 wt% HAp slip for the bimodal Porous HAp sintered body in this study was almost twice those reported in the literature [9,10]. Since the fracture of brittle materials such as ceramics is primarily a weak-link process, the micropores within the porous HAp ceramic are assumed to have no significant influence on the strength compared to that of macropores. The macropore is inherently a macro-defect in the brittle ceramic materials. The bimodal Porous L-HAp materials obtained in the study may have high-strength macropore walls, because, although the L-HAp content in the slip was relatively low, the fine L-HAp powders applied to prepare the slip were abundant in the specific surface area, and easily sintered to provide the high-strength wall support associated with the large macropores.

4. Summary

The flexural strength of porous ceramics depends on the porous framework. In this study, fine HAp particles having large specific surface area were used, and the optimum HAp powder concentration was lower than that for the other works using HAp powders of low specific surface area. But the powder having large specific surface area is easily sintered to produce a dense and firm framework, and the resultant bimodal porous HAp ceramics should show high flexural strength. The flexural strength obtained for the bimodal porous HAp sintered body was greater than that of those reported in the literature. This study shows that the bimodal pore structure of a HAp sintered body obtained could be potentially suitable for applications as a biomedical bone replacement material. As a result, it is also thought that it is possible to serve as a reference for the synthesis of a different structure porous body.

Acknowledgment

The Project Sponsored by the Scientific Research Foundation for the Returned Overseas Chinese Scholars, State Education Ministry.

References

[1] C.R. Nunes, S.J. Simske, R. Sachdeva, L.M. Wolford, Long-term ingrowth and apposition of porous hydroxylapatite implants, J. Biomed. Mater. Res. 36 (1997) 560–563.
[2] S. Joschek, B. Nies, R. Krotz, A. Göpferich, Chemical and physicochemical characterization of porous hydroxyapatite ceramics made of natural bone, J. Biomater. 21 (2000) 1645–1658.
[3] C.J. Damien, J.R. Parsons, Bone graft and bone graft substitutes: a review of current technology and applications, J. Appl. Biomater. 2 (1991) 187–208.
[4] D.M. Liu, Fabrication and characterization of porous hydroxyapatite granules, Biomaterials 17 (1996) 1955–1957.
[5] D.M. Liu, Control of pore geometry on influencing the mechanical property of porous hydroxyapatite bioceramic, J. Mater. Sci. Lett. 15 (1996) 419–421.
[6] N. Ozgur Engin, A.C. Tas, Manufacture of macroporous calcium hydroxyapatite bioceramics, J. Euro. Ceram. Soc. 19 (1999) 2569–2574.
[7] N.M.D. Pasuti, G.P.H.D. Daculsi, J.M.M.D. Rogez, S.M.D. Martin, J.V.M.D. Bainvel, Macroporous calcium phosphate ceramic performance in human spine fusion, Clin. Orthop. Relat. Res. 248 (1989) 169–176.
[8] J. Hu, J.J. Russel, B. Ben-Nissan, R. Vago, Production and analysis of hydroxyapatite from Australian corals via hydrothermal process, J. Mater. Sci. Lett. 20 (2001) 85–87.
[9] D.-M. Liu, Preparation and characterisation of porous hydroxyapatite bioceramic via a slip-casting route, Ceram. Int. 24 (1998) 441–446.

[10] T. Nakajima, Y. Tominaga, K. Yamaguchi, A. Yamamoto, M. Kouketsu, Development of hydroxyapatite ceramics as artificial bone, J. Jpn. Soc. Biomater. 17 (1999) 257–263.
[11] M. Fabbri, G.C. Celotti, A. Ravaglioli, Hydroxyapatite-based porous aggregates: physico-chemical nature, structure, texture and architecture, Biomaterials 16 (1995) 225–228.
[12] M. Fabbri, G.C. Celotti, A. Ravaglioli, Granulates based on calcium phosphate with controlled morphology and porosity for medical applications: physico-chemical parameters and production technique, Biomaterials 15 (1994) 474–477.
[13] F. Lelèvre, D. Bernach-assollant, T. Chartier, Influence of powder characteristics on the rheological behaviour of hydroxyapatite slurries, J. Mater. Sci. Mater. Med. 7 (1996) 489–494.
[14] P. Sepulveda, F.S. Ortega, M.D.M. Innocentini, V.C. Pandolfelli, Properties of highly porous hydroxyapatite obtained by the gelcasting of foams, J. Am. Ceram. Soc. 83 (2000) 3021–3024.
[15] Y. Zhang, Y. Yokogawa, T. Kameyama, Synthesis of apatite ceramics with bimodal pore structure using mechanochemically prepared fine apatite powder, Key Eng. Mater. 280–283 (2005) 1571–1574.
[16] PDF Card no. 9-432. ICDD, Newton Square, Pennsylvania, USA.
[17] A. Osaka, Y. Miura, K. Takeuchi, M. Asada, K. Takahashi, Calcium apatite prepared from calcium hydroxide and orthophosphoric acid, J. Mater. Med. 2 (1991) 51–55.
[18] I.R. Gibson, S.M. Best, W. Bonfield, Chemical characterization of silicon-substituted hydroxyapatite, J. Biomed. Mater. Res. 44 (1999) 422–428.
[19] H. Sugihara, A. Sato, F. Todaka, Y. Ikebe, K. Sugahara, The calcium phosphate products from various condensed phosphoric compounds, Gypsum & Lime 210 (1987) 292.
[20] J. Cesarano III, I. Aksay, Processing of highly concentrated aqueous α-alumina suspensions stabilized with polyelectrolytes, J. Am. Ceram. Soc. 71 (1988) 1062–1067.
[21] Y. Hirata, A. Nishimoto, Y. Ishihara, Effects of addition of polyacrylic ammonium on colloidal processing of a-alumina, J. Ceram. Soc. Jpn. 100 (1992) 983–990.
[22] Y. Zhang, Y. Yokogawa, T. Kameyama, Influence of powder particle size of slurries on mechanical properties of porous hydroxyapatite ceramics, Key Eng. Mater. 284–286 (2005) 365–368.
[23] P. Sepulveda, J.G.P. Binner, Processing of cellular ceramics by foaming and in situ polymerisation of organic monomers, J. Euro. Ceram. Soc. 19 (1999) 2059–2066.
[24] L.L. Hench, J. Wilson, An Introduction to Bioceramics, World Scientific, Singapore, Republic of Singapore, 1993.
[25] D.J. Green, P. Colombo, Cellular ceramics: intriguing structures, novel properties, and innovative applications, MRS Bull. 28 (2003) 296–300.